

Comparative study of organic metals and high- T_c cuprates

S. Barišić

Department of Physics, Faculty of Science, University of Zagreb, Bijenička c. 32, HR-10000 Zagreb, Croatia

O. S. Barišić

*Jožef Stefan Institute, SI-1000 Ljubljana, Slovenia and
Institute of Physics, Bijenička c. 46, HR-10000 Zagreb, Croatia*

The Bechgaard salts and the high T_c cuprates are described by two and three band models, respectively, with the lowest band (nearly) half filled. In organics the interactions are small, while in cuprates the repulsion U_d on the Cu site is the largest energy. The Mott AF state is stable in undoped materials in both cases. In the metallic phase of cuprates the $U_d \rightarrow \infty$ limit produces a moderate effective repulsion. The theories of the coherent SDW and charge-transfer correlations in the metallic phases of organics and cuprates are thus similar. In (undoped) organics those correlations are associated with commensurate $2k_F$ SDW and $4k_F$ bond or site modes. The corresponding modes in metallic cuprates are the incommensurate SDW and in particular O_x/O_y quadrupolar charge transfer with wave vector $2q_{SDW} = q_0 + G$. They are enhanced for dopings $x > 0$, which bring the Fermi level close to the van Hove singularity. Strong coupling to the lattice associates the static incommensurate O_x/O_y charge transfer with collinear “nematic” stripes. In contrast to organics, the coherent correlations in cuprates compete with local $d_{10} \leftrightarrow d_9$ quantum charge-transfer disorder.

I. INTRODUCTION

The high- T_c cuprates are usually described by the Emery model¹ where the role similar to the external dimerization² in the Bechgaard salts is played by the Cu-O hopping t_{pd} , which puts two oxygens in the CuO_2 unit cell and makes the lowest of three bands half filled. The weak coupling theory at zero doping x is then a quite straightforward analogue^{3,4,5,6} of the 1D theory, provided that the imperfect nesting associated with the O_x/O_y hopping t_{pp} is ignored. The appearance of the $x = 0$ Mott-AF state is essentially independent of the value of $\Delta_{pd} = \varepsilon_p - \varepsilon_d > 0$ where ε_d and ε_p are the Cu and O site energies in the hole picture, respectively.

However, while the Hubbard repulsion in the Bechgaard salts is small, in the high- T_c cuprates the repulsion U_d on the copper site is the largest energy¹. It has long been maintained^{3,4} that the fundamental question in the high- T_c cuprates concerns the nature of correlations which reduce U_d . The relevant $U_d = \infty$ limit is usually taken starting from the unperturbed state with average Cu-occupation $n_d^{(0)} = 1$. The lowest order process shown in Fig. 1a then corresponds to the fact that two holes on the neighboring Cu-sites can hop simultaneously to the intermediate O-site, empty at $x = 0$, provided that their spins are opposite. This leads to the superexchange⁷ $J_{pd} \sim t_{pd}^4/\Delta_{pd}^3$ which is the basis of the $t - J$ models⁷. Alternatively, one can assume that all holes in the unperturbed metallic state are on the O-sites, i.e., that $n_d^{(0)} = 0$. When two p -holes of opposite spin are crossing the intermediate empty Cu-site one hole hops to the Cu-site when t_{pd} is turned on, while the other has to wait as long as the Cu-site is occupied. The waiting time is of the order of $(\varepsilon_d - \mu)^{-1}$ where μ is the chemical potential of the two holes. The whole process of Fig. 1b consists of two independent $t_{pd}^2/(\varepsilon_d - \mu)$ hoppings, one

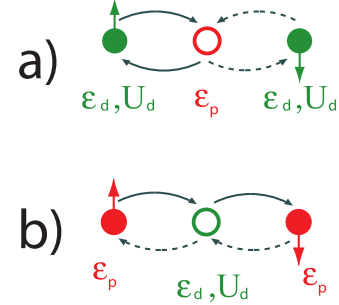


Figure 1: (Color online) (a) Superexchange of two holes on Cu sites via the empty oxygen site; (b) scattering of two holes on the O-sites via the empty Cu-site.

per particle, and of the waiting time. Therefore the resulting effective $U_d = \infty$ repulsion \tilde{U} of two p -particles is of the order of

$$\tilde{U} \sim t_{pd}^4/(\varepsilon_d - \mu)^3 \quad (1)$$

and can be interpreted as a retardation (kinetic) effect.

II. $U_d = \infty$ SLAVE PARTICLE THEORY OF THE METALLIC PHASE

We have carried out the corresponding systematic theory which starts from the $n_d^{(0)} = 0$ unperturbed metallic ground state by using the slave particles. This time dependent diagrammatic approach, of infinite order in the perturbation t_{pd} , requires the use of the spinless fermion-Schwinger boson representation in order to avoid the degeneracy of the $n_d^{(0)} = 0$ unperturbed ground state in the

overcomplete slave particle Hilbert space. The advantage of this representation is that the perturbation theory is manifestly translationally invariant at each stage, and ultimately locally gauge invariant. The disadvantage is that the three sorts of particles involved, p^σ -fermions, f -spinless fermions and Schwinger's b^σ -bosons are distinguishable, i.e., that the Cu-O anticommutation rules are replaced by commutations. The theory has to be therefore antisymmetrized *a posteriori*. Here, we only quote the results.

First, the omission of the Cu-O anticommutation rules is irrelevant in the lowest $r = 1$ order of the Dyson perturbation theory. The reason is that the Cu site is initially empty, while one particle on Cu is required for anticommutation and two for U_d interaction. This makes the $r = 1$ expression for physical single-particle propagators strictly equivalent to the result of the t_{pd} hybridized HF theory. The HF theory is expressed in terms of two hybridized propagators, one which starts and finishes with the appropriately weighted propagation on the O-sites (pdp propagator hereafter) and the other begins and ends on the Cu-sites (dpd propagator). Both propagators are characterized by the three $i = L, I, U$ bands of poles (branches) at $\omega_k^{(i)}$ ⁸. This holds irrespectively of the average HF occupation $n_d^{(1)}$ of the Cu-site associated with the chemical potential $\mu^{(1)}$. On the other hand, the relations required ultimately by the local gauge invariance $n_f + n_b = 1$ and $n_d = n_b$ are nearly satisfied at $r = 1$ only when $n_d^{(1)}$ is small, i.e., the theory then converges quickly. It is therefore important to keep in mind that^{3,6} $n_d^{(1)} \approx 1/2$ at $|x|$ small for $t_{pd} \gg \Delta_{pd}$ and that finite t_{pp} decreases it⁸ further. The overall rule of thumb is that $n_d^{(1)} < 1/2$ as long as the HF chemical potential $\mu^{(1)}$ falls below the vH singularity in the lowest L-band, i.e., as long as $x < x_{vH}$ where⁸ $x_{vH} \propto -t_{pp}$ is the positive doping required to reach the vH singularity. As easily seen, small $n_d^{(1)}$ corresponds to a weak effective interaction $\tilde{U} < t_{pd}$.

The Cu-O (anti)commutation rules are also irrelevant for two further $r = 2, 3$ expressions. $r = 2$ leads to the coherent Brinkmann-Rice-like band narrowing $t_{pd}^2 \rightarrow t_{pd}^2(1 + n_d/2)(1 - n_d)$ and the variation of Δ_{pd} through $\varepsilon_d \rightarrow \tilde{\varepsilon}_d$. However, unlike in the mean-field^{8,9,10} slave particle approximations, this is accompanied by the incoherent, local, dynamic fluctuations identified as the $d_{10} \leftrightarrow d_9$ charge-transfer disorder. Importantly, the disorder falls far from the Fermi level, although there are indications^{10,11,12} that in higher perturbation orders it spreads all over the spectrum.

The interaction \tilde{U} appears explicitly for $r = 4$. It introduces the particle-particle and particle-hole correlations in the single particle pdp and dpd propagations. $\tilde{U} > 0$ favors the coherent particle-hole correlations which appear here as pseudogaps. The slave fermion theory predicts however that the effect of \tilde{U} is the same in the singlet and the triplet channels, which is the con-

sequence of the omission of the Cu-O anticommutation rules. The *a posteriori* antisymmetrization of the theory therefore associates \tilde{U} with the singlet (SDW) scattering only.

The relevant SDW hole-electron correlations are associated to lowest order with the $pdp - pdp$ bubble, as suggested by Fig. 1b, where \tilde{U} appears as the effective interaction between p -particles. In contrast, the corresponding small U_d theory^{3,5,6} involves the $dpd - dpd$ bubble. However, although the spectral densities of the pdp and dpd propagators are complementary, the poles are the same. The associated elementary intraband bubbles share therefore the properties of the overlap of the vH singularities and of the (imperfect) Fermi surface (FS) nesting, which both favor the coherent SDW fluctuations with a dominant \vec{q}_{SDW} .

As mentioned above, $\mu^{(1)}$ in the vicinity of the vH singularity brings the metallic $U_d = \infty$ theory into the intermediate $\tilde{U} \approx t_{pd}$ regime with $n_d^{(1)} \approx 1/2$. Various experiments and NQR in particular¹³ indicate indeed that for $|x| \leq 0.2$ the average occupation of the Cu site is close to $n_d \approx 1/2$. Therefore, we associate the transition, between the $|x| \approx 0$ long- and short-range magnetic order and the metallic phase at finite $|x|$, to the crossover in x between the $|x| \approx 0$ $t - J$ regime and the finite $|x|$ metallic regime considered here. This latter is characterized by the close competition of the $d_{10} \leftrightarrow d_9$ charge-transfer disorder and the coherence effects which is difficult to cover analytically. In this light, we shall identify below the physical content of the important hole-electron correlation functions and determine when their coherent limit is consistent with experiments in the metallic phase.

III. COHERENT E-H CORRELATIONS AND STRIPES

Let us start with the SDW correlations for $x \approx x_{vH} > 0$. The vH overlap/FS nesting behavior of the elementary intraband particle-hole bubble is not universal. It is however well known that $\text{Re}\chi_{SDW}^{L,L}(\vec{q}, \omega)$ becomes large for ω small and close to π/a [1, 1]. Taking formally $t_{pp} = 0$, the log square singularity in ω occurs^{3,5} at $x = 0$ due to the vH overlap and to the perfect 2D FS nesting at $\vec{q}_{SDW} = \pi/a$ [1, 1]. Analytical¹⁴ and numerical¹⁵ calculations show that imperfect nesting associated with finite x at $t_{pp} = 0$ produces spikes at incommensurate \vec{q}_{SDW}^{coll} along the zone main axes. With finite t_{pp} the spikes were also obtained numerically¹⁶ for \vec{q}_{SDW}^{dg} along its diagonals. While it seems well established¹⁷ that the spikes at \vec{q}_{SDW}^{coll} are dominated by the pairing of holes and electrons close to the antinodal π/a [1, 0] and π/a [0, 1] vH points, the pairing which gives rise to the spikes at \vec{q}_{SDW}^{dg} is not yet determined unambiguously.

The single well-defined collinear $\pm\vec{q}_{SDW}^{coll}$ leg or the nearly circular $|\vec{q}_{SDW}|$ is observed clearly by the magnetic neutron scattering^{18,19,20}. As a rule, \vec{q}_{SDW}^{coll} appears for small energy transfers while $|\vec{q}_{SDW}|$ occurs at high

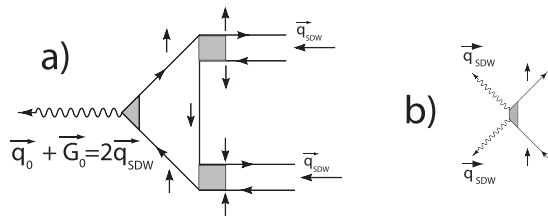


Figure 2: Umklapp coupling of two SDW's enhanced at \vec{q}_{SDW} (a) to intracell charge fluctuations and/or to phonons linearly coupled to carriers; (b) to phonons coupled quadratically to the carriers. Internal structure of the electronic triangle is governed by the A_g , B_g symmetry properties of the outgoing vertices and by the U_d and \bar{U} nature of the incoming square vertices which flip the spins.

frequencies e.g. in metallic YBCO¹⁹. The observation of the strong leading harmonics is consistent with metallic coherency in the propagation of t_{pd} -hybridized particles. There is however also good NMR evidence²¹ that non-magnetic disorder is present in LSCO. It may well correspond, in part, to the local $d_{10} \leftrightarrow d_9$ charge disorder, which is dynamic in the present theory but becomes frozen^{21,22} by the strong coupling²³ to the heavy lattice.

The Emery model also encompasses²³ the Cu/O₂ and O_x/O_y charge transfers and various bond fluctuations within the unit cell. In the $\vec{q} \rightarrow 0$ limit the D_4 symmetry classifies^{24,25,26} those correlations in A_{1g} , B_{1g} and B_{2g} irreducible representations, the bond fluctuations being involved directly²⁶ into the Raman responses. The elementary bubbles associated with those correlations differ through coherence factors in their numerators while their respective poles and integration ranges are the same²⁶. The $\vec{q} = 0$ $B_{1g,2g}$ modes are dominated²⁶ respectively by the contributions from the main axes or diagonals of the CuO₂ zone. They have their own small \vec{q} structures^{15,16} (e.g. the elementary O_x/O_y bubble is logarithmically singular^{3,23} at $x = x_{vH}$). In addition, while the $\vec{q} \approx 0$ B_{1g} and B_{2g} intracell modes are decoupled from the $\vec{q} \approx 0$ transfers of the total CuO₂ charge among the distant unit cells^{15,23,26}, the coherent $\vec{q} \approx 0$ Cu/O₂ charge transfer is accompanied^{15,26} by the $\vec{q} \approx 0$ intercell charge transfer. Only the latter is subject to the long range Coulomb screening/frustration^{15,22,26,27}.

The small \vec{q} behavior of the charge transfer correlations is however of secondary interest if the SDW is taken¹⁴ as the dominant fluctuation. Then, according to Fig. 2, two SDW's enhanced at $\vec{q}_{SDW} \approx \pi/a [1, 1]$ either couple to the intracell fluctuations and then to phonons, or else directly to phonons. In the case of linear coupling of Fig. 2a the corresponding dominant \vec{q}_0 is small and satisfies the physically important relation

$$\vec{q}_0 + 2\pi/a [1, 1] = 2\vec{q}_{SDW} . \quad (2)$$

Alternatively, as in Fig. 2b, two such SDW's can also couple quadratically²³ to tilts of the CuO₆ octahe-

dra at $\vec{q}_{TILT} = \vec{q}_{SDW}$. When two SDW's enhanced at \vec{q}_{SDW}^{coll} close to $\pi/a [1, 1]$ are associated with the $\pi/a [1, 0], \pi/a [0, 1]$ pairing they drive²⁶, directly or via the B_{1g} O_x/O_y charge transfer, the LTT/($e_{xx}-e_{yy}$) deformations at $\pm\vec{q}_{TILT}^{coll}/\pm\vec{q}_0^{coll}$. Analogously, if two SDW's enhanced at \vec{q}_{SDW}^{dg} close to $\pi/a [1, 1]$ are associated with the $\pi/a [1/2, 1/2], \pi/a[-1/2, -1/2]$ pairing they drive²⁶ the B_{2g} O_x-O_y bond fluctuations and the LTO/($e_{xy}+e_{yx}$) modes at $\pm\vec{q}_{TILT}^{dg}/\pm\vec{q}_0^{dg}$.

The $\vec{q}_{TILT} \approx \pi/a [1, 1]$ tilts and the \vec{q}_0 modes are in addition entangled²⁸ by the ionic forces, namely the $\pi/a [1, 1]$ LTT and LTO tilts are accompanied, respectively, by the *homogeneous* $e_{xx}-e_{yy}$ and $e_{xy}+e_{yx}$ shears of the CuO₂ planes. Those entangled single leg deformations thus lift, through the electron-phonon couplings²³, the degeneracy of two O_x/O_y sites²³ or of four t_{pp} bonds within the CuO₂ unit cell by dimerizing them two by two.

The stability of the striped structures can be investigated using the related^{14,23} Landau functionals. E.g., the entangled collinear modes are related in this way to the collinear nematic static stripes^{27,29} usually characterized by \vec{q}_0^{coll} . It appears thus quite clearly that the coherent O_x/O_y charge transfer, coupled to the lattice, is an essential ingredient of the collinear stripes²⁷ in the metallic phase. This agrees with observations^{18,19,24,25,30,31}. The collinear SDW and O_x/O_y charge transfer correlations get enhanced in metallic lanthanum cuprates for dopings $x \approx x_{vH}$. The spikes¹⁷ at \vec{q}_{SDW}^{coll} in $\chi_{SDW}^{LL}(\vec{q}, \omega)$ then explain the "nematic" version of Eq. (2) observed^{18,24} in the metallic phase. The corresponding LTO/LTT lattice instability is predicted²³ and observed^{32,33} to be of the first order in LBCO for $x \approx x_{vH} \approx 1/8$. Those effects are attributed here to the vH overlap/FS nesting, while the commensurability 1/8 is expected to play only the secondary role.

In contrast to lanthanum cuprates the Fermi level μ in the optimally doped YBCO and BSCO, as measured by ARPES, falls⁸ well below the vH point, i.e., $x < x_{vH}^{HTC}$. The collinear SDW-O_x/O_y stripes enhanced by the vH singularities are therefore not expected to occur in metallic YBCO and BSCO. Indeed, at larger x , the collinear stripe structure is replaced²⁵ by the fourfold commensurate stripes in "checkerboard" configuration^{25,34}, which restores the D_4 symmetry.

The salient new feature of the present low-order large U_d analysis is thus that the coherent, weak, incommensurate collinear¹⁷ SDW and O_x/O_y correlations appear to get enhanced with respect to the $d_{10} \leftrightarrow d_9$ charge disorder if the vH singularities are reached³⁵ by doping x_{vH} . This explains the long standing puzzle³² why the enhanced magnetic/charge coherence occurs twice in LBCO as a function of doping, once as the long- or short-range^{4,36} AF order at $x \approx 0$ and then again as the incommensurate SDW at single $\pm\vec{q}_{SDW}^{coll}$ for finite positive $x_{vH} \approx 0.1$, accompanied by the static O_x/O_y charge transfer coupled to the staggered LTT tilting of the CuO₄ octahedra.

Acknowledgments

Invaluable discussions with J. Friedel, L.P. Gor'kov, I. Kupčić, D.K. Sunko and E. Tutiš are gratefully ac-

knowledged. This work was supported by the Croatian Government under Projects No. 119 – 1191458 – 0512 and No. 035 – 0000000 – 3187.

-
- ¹ V.J. Emery, Phys. Rev. Lett. 58 (1987) 2794.
² S. Barišić, S.Brazovskii, Recent Developments in Condensed Matter Physics ed. J.T. Devreese (Plenum, New York) Vol. 1 (1981) 327.
³ J. Friedel, J. Phys. Cond. Matt. 1 (1989) 7757.
⁴ J. Friedel, M. Kohamoto, Eur. Phys. J. B 30 (2002) 427.
⁵ I.E. Dzyaloshinskii, V.M. Yakovenko, ZhETF 94 (1988) 344.
⁶ S. Barišić, I. Batistić, Physica Scripta. T 27 (1989) 78.
⁷ F.C. Zhang, T.M. Rice, Phys. Rev. B 37 (1987) 3759.
⁸ I. Mrkonjić, S. Barišić, Eur. Phys. J. B 34 (2003) 69.
⁹ G. Kotliar, P.A. Lee, N. Read, Physica C 153-155 (1989) 538.
¹⁰ L. Janković, D.K. Sunko, Physica C 341-348 (2000) 2103.
¹¹ H. Nikšić, E. Tutiš, S. Barišić, Physica C 241 (1995) 247.
¹² M.B. Zöfl, Th. Maier, Th. Pruchke, J. Keller, Eur. Phys. J. B 13 (2000) 47.
¹³ I. Kupčić, S. Barišić, E. Tutiš, Phys. Rev. B 57 (1998) 8590.
¹⁴ H.J. Schulz, Phys. Rev. Lett. 64 (1990) 1445.
¹⁵ E. Tutiš, H. Nikšić, S. Barišić, Lecture Notes in Physics 427, (1997) 1 (Springer Verlag).
¹⁶ J.-H. Xu, T.J. Watson-Yang, J. Yu, A.J. Freeman, Phys. Lett. A 120 (1987) 489.
¹⁷ Q. Si, Y. Zha, K. Levin, Phys. Rev. B 47 (1993) 9055.
¹⁸ J.M. Tranquada *et al*, Nature 429 (2004) 534.
¹⁹ C. Stock *et al*, Phys. Rev. B 71 (2006) 024522.
²⁰ V. Hinkov *et al*, Science 319 (2008) 597.
²¹ L.P. Gor'kov, G.B. Teitel'baum, cond-mat/0801.1728.
²² L.P. Gor'kov, A.V. Sokol, JETP Lett. 46 (1987) 420.
²³ S. Barišić, J. Zelenko, Sol. St. Comm. 74 (1990) 367.
²⁴ A.G. Gozar *et al*, Frontiers in Magn. Materials, 755, Springer-Verlag (2005).
²⁵ L. Tassini, W. Prestel, A. Erb, M. Lambacher, R. Hackl, PRB 78 (2008) 020511(R).
²⁶ I. Kupčić, S. Barišić, Phys. Rev. B 75 (2007) 094508, and to be published.
²⁷ S.A. Kivelson *et al*, Rev. Mod. Phys. 75 (2003) 1201.
²⁸ B. Piveteau, C. Nougera, Fizika 21 (1989) 237.
²⁹ V.J. Emery, S.A. Kivelson, Physica C 209 (1993) 597.
³⁰ A. Bianconi *et al*, Phys. Rev. Lett. 76 (1996) 3412.
³¹ S. Sugita, T. Watanabe, A. Matsuda, Phys. Rev. B 62 (2000) 8715.
³² J.D. Axe *et al*, Phys. Rev. Lett. 62 (1989) 2751.
³³ H. Kimura *et al*, J. Phys. Soc. Jpn. 74 (2005) 445.
³⁴ T. Hanaguri *et al*, Nature 430 (2004) 1001.
³⁵ A. Ino *et al*, Phys. Rev. B 65, (2002) 094504.
³⁶ J. Lorenzana, G.A. Sawatzky, Phys. Rev. B 52 (1995) 9576.